

NUMERICAL STUDY ON THE FLEXURAL PERFORMANCE OF RC BEAMS WITH EXTERNALLY BONDED CFRP SHEETS

Nguyen Ngoc Tan^{a,*}, Nguyen Trung Kien^a, Nguyen Hoang Giang^a

^a*Faculty of Building and Industrial Construction, Hanoi University of Civil Engineering, 55 Giai Phong road, Hai Ba Trung district, Hanoi, Vietnam*

Article history:

Received 21/7/2021, Revised 20/10/2021, Accepted 21/10/2021

Abstract

The numerical investigations on the structural performance of reinforced concrete (RC) beam strengthened with externally bonded carbon fiber-reinforced polymer (CFRP) sheets are presented. The nonlinear characteristics of materials (i.e., stress-strain relationships of steel reinforcement, concrete, CFRP, and CFRP/concrete bond stress-slip behavior) were adopted in three-dimensional finite element (FE) models. The validation of FE models was conducted by comparing the laboratory works carried out on two RC beam specimens with 2000 mm length, 300 mm height, and 120 mm width. The numerical results show a good correlation with the experimental results of the beam specimens, such as load-displacement curves, crack patterns, and failure modes. They allow confirming the capability of the developed FE model to predict the flexural performance of strengthened beams considering CFRP/concrete interfacial behavior. Furthermore, parametric investigations were performed to determine the effect of flexural strengthening schemes, CFRP length with or without U-wraps, and multiple CFRP layers on the flexural performance of strengthened beams.

Keywords: reinforced concrete beams; flexural strengthening; flexural performance; bond-slip behavior; carbon fiber-reinforced polymer.

[https://doi.org/10.31814/stce.huce\(nuce\)2021-15\(4\)-16](https://doi.org/10.31814/stce.huce(nuce)2021-15(4)-16) © 2021 Hanoi University of Civil Engineering (HUCE)

1. Introduction

Nowadays, the need to strengthen and rehabilitate existing reinforced concrete (RC) structures has increased over the decades. It is often due to the original design limits, construction errors, progressive damages under aggressive environmental conditions [1–3]. Therefore, various retrofitting methods have been investigated and developed, e.g., waterproofing, jacking the deteriorated structural members to maintain or even improve their load-carrying capacity, strengthening RC structures using fiber-reinforced polymer (FRP), etc. As a result, the growing popularity of utilizing FRP materials based on externally bonded techniques strengthens RC structures. Moreover, FRP materials are applicable to many kinds of structures, i.e., column, beam, wall, slab. It is mainly due to the superior mechanical properties of FRP materials, such as a high strength-to-weight ratio, lightweight, easy installation, excellent corrosion resistance [4]. Generally, there are three typical schemes to apply FRP sheets externally bonded for strengthening RC beams: (i) side-bonded on the opposite lateral faces, (ii) bottom-bonded on the bottom face, and (iii) completely wrapping [5–7].

*Corresponding author. *E-mail address:* tannn@nuce.edu.vn (Tan, N. N.)

The effectiveness of FRP strengthening on the structural performances of RC beams has been experimentally studied and discussed in many research works [8–10]. For instance, the experiments conducted by Dong et al. [9] showed that the overall flexural and shear capacity of CFRP-strengthened beams increased by at least 30% as to control beams. Furthermore, the advantages of using thin CFRP sheets are not only the improvement of both beam stiffness and ductility but also to control the development of cracks. In addition to focusing on reinforcing the RC beams designed specifically to fail by shear or flexural failure, the application of flexural-shear strengthening FRP sheets demonstrated an even more considerable increase in load carrying, initial stiffness, and hardening behavior of the strengthened beams. However, it is well known that despite the capability of achieving considerable increases in strength capacities, a critical concern of RC structures strengthened with externally bonded FRP sheets is the premature failure by FRP delamination or debonding [11–13]. Therefore, in order to achieve the successful design of both shear and flexural strengthening using FRP, it is important to predict such debonding failure.

The finite element method (FEM) is a numerical approach due to its extreme effectiveness in analyzing engineering problems, especially complex boundary conditions. Therefore, several numerical studies using FEM have been conducted on the topic of FRP-strengthened RC beams [14–21]. The developed FE models adapted in these studies have been able to give good results in terms of load-carrying capacity, initial stiffness, as well as failure modes. However, the design-oriented parameters that significantly affect the performance of strengthened RC beams have not been analyzed thoroughly. There is a limited number of researches on the influence of FRP length and the use of U-wraps providing anchorage systems. The study conducted by Hawileh et al. [22] indicated that U-wrap anchorages increase the total capacity of the beam while also increasing its ductility. However, the anchorage mechanism has been shown to have no effect on the flexural strength of strengthened beams. It is also stated in the experimental study by Ali et al. [1].

Furthermore, various bonding schemes can be used and considered as an influencing factor on the strengthening performance. For example, the study conducted by Salama et al. [23] investigated the flexural performance of RC beams strengthened with side-bonded CFRP and indicated that the side-bonded technique boosts flexural strength by 39.7-93.4 percent. Additionally, it is stated that the side-bonded technique is slightly less effective than externally bonding in the tension surface. Meanwhile, Sobuz et al. [24] conducted an experimental study to determine the influence of FRP layers on stiffness and flexural strength. They discovered that multiple layers increase stiffness and flexural strength. However, the research concerning the number of FRP layers is still limited due to the complexity of experiments, and further work is necessary to gain insight into this aspect.

In this paper, two beam specimens have been studied to investigate the flexural performance of RC beams strengthened with carbon fiber-reinforced polymer (CFRP) sheets and the interfacial behavior between CFRP and concrete. Then, a bond-slip model was used in nonlinear finite element modeling to investigate this aspect further. The validation of the simulation was based on comparing with the experimental results, including the load-displacement relationship, crack pattern, and failure mode. Finally, the numerical results have been extended with parametric investigations considering the contribution of the flexural strengthening schemes, CFRP length and U-wraps, and multiple CFRP layers on the flexural performance of strengthened beams.

2. Finite element model of RC beam specimens

2.1. Description of the experimental beam specimens

In order to verify the capability of the FE model in the present study, the validation is performed by calibrating with experimental results obtained from research work by El-Ghandour [5]. Two simply supported beams named B1 and B1F with the dimensions of $2000 \times 120 \times 300$ mm were loaded monolithically in three-point bending tests up to failure.

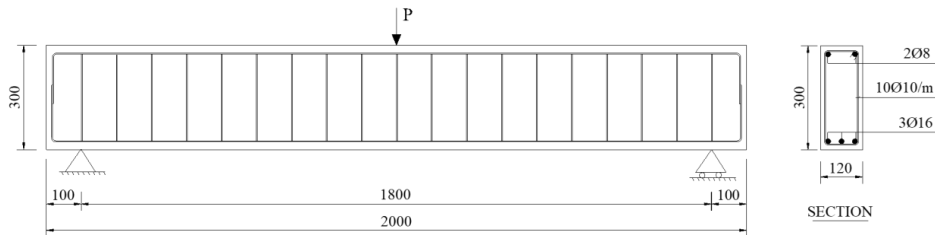


Figure 1. Detailed layout of the control beam B1

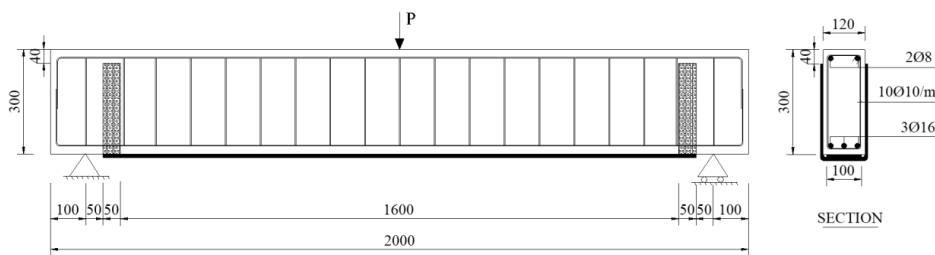


Figure 2. Detailed layout of the flexural-strengthened beam B1F

Each flexural-critical beam specimen had three steel bars at the bottom layer, two steel bars at the top layer, and stirrups with a regular spacing of 100 mm having the nominal diameters of 16 mm, 8 mm, and 10 mm, respectively, as illustrated in Fig. 1. Meanwhile, Fig. 2 shows the strengthened beam specimen externally bonded at the tension fiber with a CFRP sheet having 100 mm wide, 1700 mm length, and 0.176 mm thickness. The mechanical properties of the materials used are summarized in Table 1. Moreover, the longitudinal CFRP reinforcement was also anchored using U-wraps having 50 mm width at the plate ends. While the existing design code does not incorporate U-wrap anchorage systems when predicting the load capacity of flexural-strengthened beams, they are nonetheless beneficial in improving the maximum debonding load.

2.2. Finite element modeled beam specimens

A displacement-controlled nonlinear load-deformation analysis of CFRP strengthened RC beams is carried out using DIANA FEA software [25]. In analyses, the three-dimensional models were created consisting of a concrete beam, CFRP sheets, longitudinal and transverse reinforcement, rigid steel plates added at loading and support points to avoid stress concentration problems. The typical finite element mesh size was maintained at approximately $30 \times 30 \times 30$ mm, where the mesh discretization and the boundary conditions are shown in Fig. 3. The material constitutive models are presented in Fig. 4 for concrete, steel reinforcement, CFRP sheets, and CFRP/concrete interface. The

parameters assigned in the FE model are shown in Table 1 based on the experiment [5], simplified bond-slip model proposed by Lu et al. [12], fib Model Code 2010 [26], and formula proposed by Nakamura and Higai [27] for the compressive fracture energy of concrete.

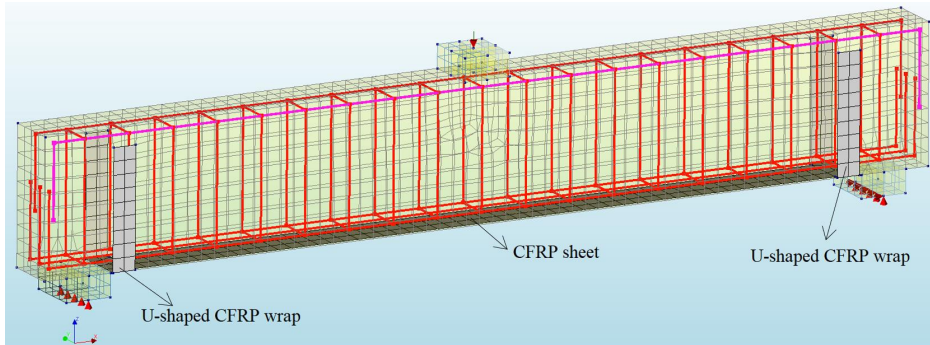


Figure 3. Finite element model components of the strengthened beam

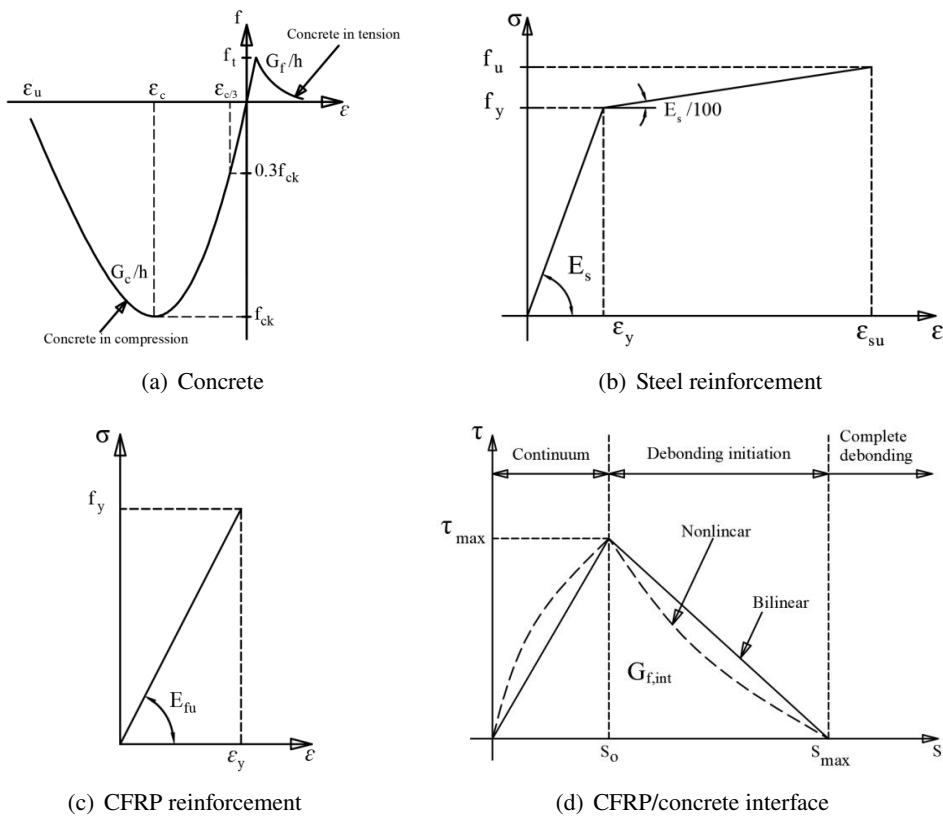


Figure 4. Material constitutive models used in the finite element modeling

Table 1. Parameters assigned in the FE model

Parameter	Symbol (Unit)	Values		Ref.
		Beam B1	Beam B1F	
Concrete compressive strength	f_{ck} (MPa)	39.5	39.5	[5]
Concrete tensile strength	f_t (MPa)	3.45	3.45	[26]
Modulus of elasticity of concrete	E_c (GPa)	30.7	30.7	[26]
Tensile fracture energy	G_f (Nmm/mm ²)	0.089	0.089	[26]
Compressive fracture energy	G_c (Nmm/mm ²)	22.25	22.25	[27]
Yield/ ultimate tensile strength of steel	$\Phi 8$ mm	290/420	290/420	[5]
	f_y/f_u (MPa) $\Phi 10$ mm	400/600	400/600	[5]
	$\Phi 16$ mm	400/600	400/600	[5]
Modulus of elasticity of steel	E_s (GPa)	200	200	[5]
Tensile strength of CFRP	f_y (MPa)	-	3800	[5]
Modulus of elasticity of CFRP	E_{fu} (GPa)	-	240	[5]
Ultimate tensile strain of CFRP	ε	-	0.0155	[5]
CFRP/concrete bond strength	τ_{max} (MPa)	-	4.3	[12]
Corresponding slip	S_0 (mm)	-	0.055	[12]

2.3. Finite element modeling

a. Concrete modeling

In order to model the concrete beam, a twenty-node isoparametric solid brick element (a three-dimensional CHX60 element) was employed. Then, the rotating crack model based on total strain was implemented with the smeared crack concept of concrete. The concrete behavior in tension was modeled using a nonlinear tension softening stress-strain relationship of Hordijk et al. [28], which was defined by the peak tensile strength, mode-I tensile fracture energy, and crack bandwidth of the element. For compression, the parabolic stress-strain curve, as illustrated in Fig. 4(a), is utilized, with the capability to consider the reduction model due to lateral cracking and the stress confinement model [25]. The strain ε_c at which the compressive strength reaches its highest value can be calculated by Eq. (1).

$$\varepsilon_c = -\frac{5}{3} \frac{f_{ck}}{E} \quad (1)$$

The corresponding strain where one-third of the maximum compressive strength f_{ck} is reached, which is calculated by Eq. (2) as follows:

$$\varepsilon_{c/3} = -\frac{1}{3} \frac{f_{ck}}{E} \quad (2)$$

Finally, the ultimate strain ε_u is determined as Eq. (3), which is the point at which the material totally softened in compression.

$$\varepsilon_u = \varepsilon_c - \frac{3}{2} \frac{G_c}{hf_{ck}} \quad (3)$$

The area under the stress-strain response of the concrete curves in compression and tension employing mode-I fracture energy and crack bandwidth can be calculated [26, 27]. Additionally, it is noted that ε_c is determined independently of the element size or compressive fracture energy [25].

b. Steel reinforcement modeling

The longitudinal and transverse reinforcements were modeled individually as embedded bar elements in the CHX60 concrete elements. The strains were estimated using the surrounding continuum elements' displacement field. The perfect bond assumption between steel reinforcement and concrete can be used in FE analysis of testing beams if the bond stress-slip behavior does not control the failure mode.

The reinforcing rebars had an elastoplastic behavior, defined by the yield strength and ultimate tensile strength indicated in Table 1. A yield plateau is followed by a strain-hardening behavior up to failure. The tangent modulus required for the strain-hardening behavior of steel reinforcement is set to one-hundredth of the modulus of elasticity, as shown in Fig. 4(b).

c. Rigid loading and support steel plates modeling

Fig. 3 illustrates the FE model, where the CHX60 element was also used for rigid steel plates. Steel class with linear elastic isotropic material properties were used in which Young's modulus and Poisson's ratio were required.

d. CFRP modeling

The CQ40S element is an eight-node quadrilateral isoparametric curved shell element that was used to model the CFRP sheets. The CFRP sheets have a very high unidirectional tensile strength but with a smaller stiffness than steel. The behavior of an orthotropic linear elastic material was employed, as illustrated in Fig. 4(c). The strain level in CFRP sheets was logged at each load step up to a maximum strain of 0.0155 [5]. Once the maximum strain in the element is reached, the RC beam is assumed to fail in a brittle mode of CFRP rupture suddenly.

e. CFRP/concrete interface modeling

The bond-slip models developed by Lu et al. [12] between the local shear stress (denoted τ) and the associated slip (denoted s) are used to simulate the CFRP/concrete interfacial behavior, as illustrated in Fig. 4(d). In a three-dimensional design, the CQ48I element has been used to model an interface element between two planes with a zero thickness. Where the nonlinear shear stress-slip behavior is defined in the ascending and descending branches as follows:

$$\tau = \tau_{\max} \sqrt{\frac{S}{S_0}} \quad \text{if } S \leq S_0 \quad (4)$$

$$\tau = \tau_{\max} e^{-\alpha\left(\frac{s}{s_0}-1\right)} \quad \text{if } S \geq S_0 \quad (5)$$

where the maximum shear stress τ_{\max} is governed by the concrete tensile strength (f_t) and the CFRP width ratio factor (β_w), and they were taken as follows:

$$\tau_{\max} = 1.5\beta_w f_t \quad (6)$$

$$\beta_w = \sqrt{\frac{2.25 - \frac{b_f}{b_c}}{1.25 + \frac{b_f}{b_c}}} \quad (7)$$

in which b_f and b_c are equal to the width of the CFRP sheet and concrete beam, respectively.

The corresponding slip S_0 of τ_{\max} is also dependent on the concrete tensile strength and the CFRP width ratio factor. The debonding process is described by a linear softening function that connects the ultimate slip S_{\max} to the interfacial fracture energy G_f . The factor α can be derived as follows:

$$S_0 = 0.0195\beta_w f_t \tag{8}$$

$$G_{f, \text{int}} = 0.308\beta_w^2 \sqrt{f_t} \tag{9}$$

$$\alpha = 1 / \left(\frac{G_{f, \text{int}}}{\tau_{\max} S_0} - \frac{2}{3} \right) \tag{10}$$

$$S_{\max} = \frac{2G_{f, \text{int}}}{\tau_{\max}} \tag{11}$$

In order to anticipate the debonding of CFRP sheet from the adjacent concrete surface, if the CFRP/concrete interface total traction (denoted τ_{int}) reaches the maximum local bond stress ($\tau_{\text{int}} = \tau_{\max}$), then the structural performance of RC strengthened beam corresponds to the initial stage of CFRP debonding failure mode. Complete debonding occurs when the slip value exceeds S_{\max} .

3. Validation of finite element models

Two beam specimens were subjected to three-point bending tests and later analyzed using the numerical approach employing the finite element method as described above. In order to validate the capability of finite element-based models in simulating the behavior of the experimentally tested beams, three criteria from the experimental and numerical results were compared, i.e., load-displacement response, crack pattern, strain development in CFRP sheets.

Table 2. Comparison of the experimental and numerical results

Specimen	Ultimate load P_u (kN)		Ratio $P_{u, \text{EXP}}/P_{u, \text{FEM}}$	Failure mode
	EXP	FEM		
Beam B1	155	157.1	0.99	Flexure
Beam B1F	170	174.7	0.98	CFRP rupture

As a result, the load-displacement curves observed in the bending test and FEM are drawn in Fig. 5 to compare the experimental and numerical results. In addition, Table 2 synthesizes and compares the predicted and experimentally measured ultimate load (denoted P_u) along with the failure mode. In terms of maximum load-carrying capacities in beams B1 and B1F, the ratio of the numerical-to-experimental load capacity indicated a good agreement between the testing and FEM. However, the modeled beam specimens using smeared crack model exhibited a higher initial stiffness, which can be explained by the stress locking behavior in the cracked element [29].

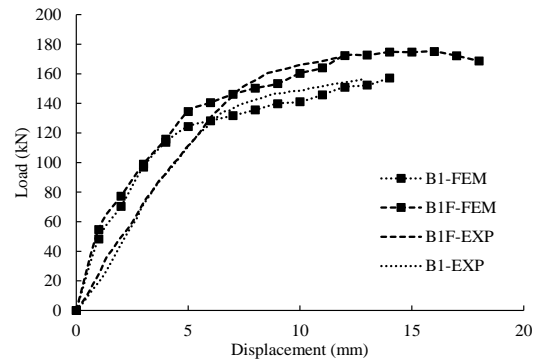


Figure 5. Comparison of load-displacement curves between experiment and FEM

In addition, the failure modes of tested beams can also be captured employing the developed finite element model. As shown in Fig. 6, the Cauchy stress obtained in longitudinal reinforcement and the Cauchy total stresses distributed over the concrete beam has exceeded the yield strength of 400 MPa and concrete compressive strength of 39.5 MPa, respectively, at the failure step of the analysis. Therefore, it is capable of representing the ductile manner of flexural failure in the control beam B1.

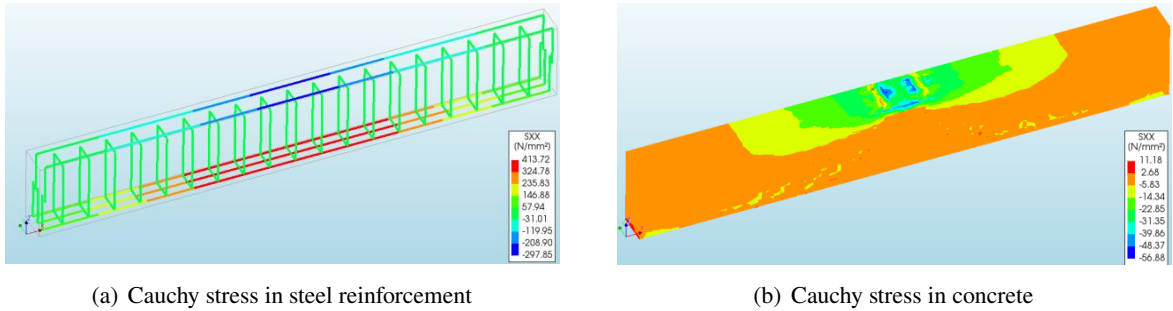


Figure 6. FE analysis for simulated beam B1-FEM (non-strengthened beam)

For the case of simulated strengthened beam B1F-FEM, the interfacial shear stress distribution (noted ISSD) at the CFRP/concrete interface and CFRP strain distribution (noted CSD) at beams' displacement of 16 mm in Fig. 7 showed that the total traction on the interface element had not reached the CFRP/concrete bond stress. Meanwhile, the element strain in the longitudinal direction of the CFRP sheet exceeded the maximum strain of 0.0155. Hence, the obtained results confirmed that the failure mode of the CFRP sheet in the middle span is similar to the experiment.

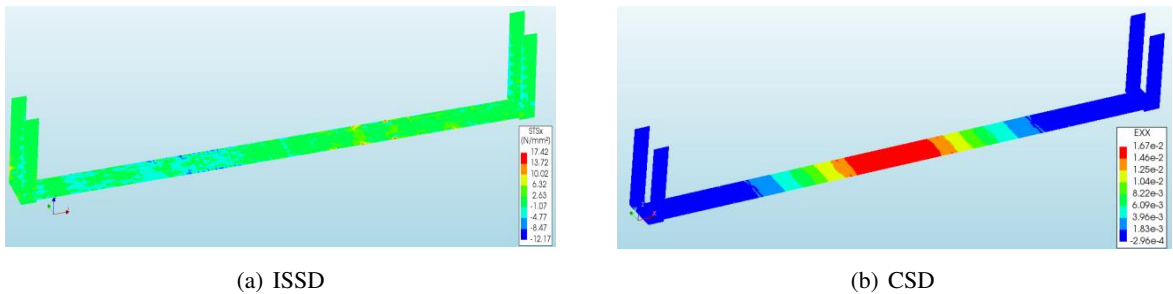


Figure 7. Interfacial shear stress and strain distribution in the longitudinal axis of CFRP sheet

In Fig. 8, the crack strain distribution obtained at the failure stage of two simulated beams employing FEM also shares the same patterns as it provided in the experiment. Thus, the similarity of the crack patterns also further confirms the capability of the developed FE model in predicting the structural performance of unstrengthened and CFRP strengthened RC beams.

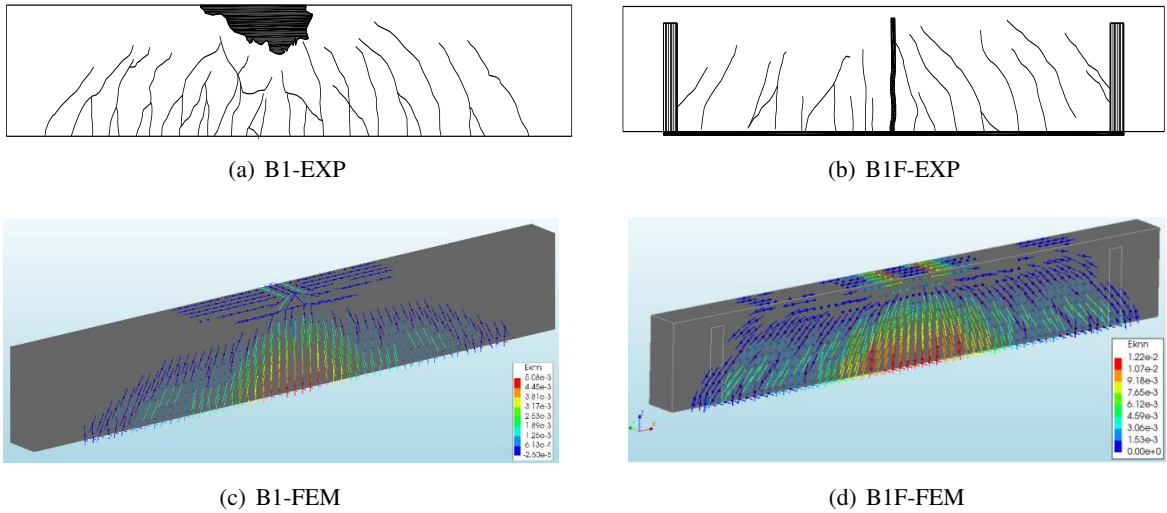


Figure 8. Comparison of crack patterns between experiment and FEM

4. Parametric study

The literature review indicates that although substantial research has been conducted on CFRP strengthening of RC beams, the behavior of CFRP/concrete interfacial behavior under different schemes of strengthening on the structural performance of strengthened beams was not well elaborated. Hence, the parametric study is herein performed by developing and analyzing five additional FE models to study the effect of strengthening schemes, length, and layer number of CFRP sheets on the structural performance of strengthened RC beams as well as on the CFRP/concrete interfacial behavior.

4.1. Effect of flexural strengthening schemes

Three FE models were developed to further investigate the flexural behavior of strengthened beams when the strengthening schemes are changed. In the case of beam B1F-FEM, the CFRP longitudinal sheet was externally bonded to the tension surface, and the CFRP U-wraps were additionally attached at the ends (cf. Fig. 2). The second scheme refers to the beam named B1F-WU, which has been modeled without the U-wrap anchorages, as shown in Fig. 9(a). Finally, the sided bonding scheme, as shown in Fig. 9(b), has been applied for modeled beam named B1F-SB, where the two CFRP sheets of 1700 mm length, 50 mm width, and 0.176 mm thickness were bonded to the two opposite lateral sides of the beams' web, as they act like tensile steel reinforcement.

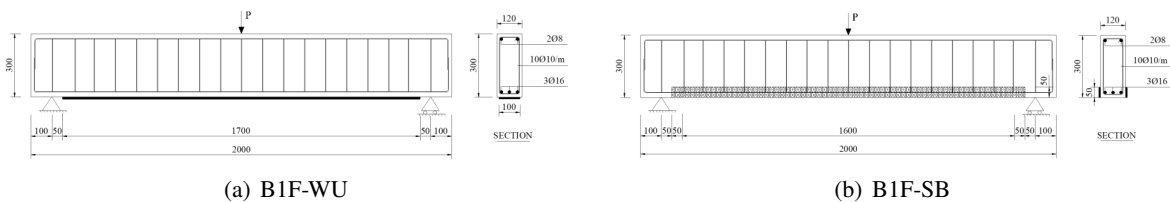


Figure 9. Modeled beams strengthened with bottom-bonded and side-bonded CFRP sheets

Fig. 10 indicated the load-displacement response of three investigated beams consisting of B1F-FEM, B1F-WU, and B1F-SB. The overall behavior of two beams with or without the U-wrap end anchorages exhibited around 6% difference in maximum load-carrying capacity with much higher ductility than beam B1F-SB due to the different failure mechanisms. U-wrap anchorage in beam B1F-FEM led to an approximately 5.4% increase to beam B1F-WU.

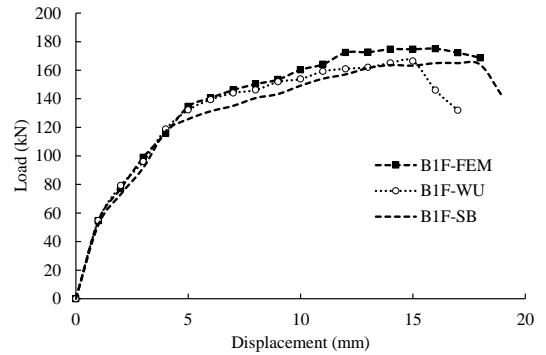


Figure 10. Load-displacement response of modeled beams with various flexural strengthening schemes

In order to investigate further the interfacial behavior of beam specimens, the shear stress distributions of beam B1F-WU and beam B1F-SB along with the interface are illustrated in Fig. 11.

As in beam B1F-FEM, the beam failed due to the CFRP rupture in the tension area. Furthermore, the failure mode of beam specimen B1F-WU obtained from FE analysis was debonding. At the failure stage, the delamination of the CFRP sheet appeared near the intermediate span, as shown in Fig. 12(a), since the shear stress on the interface was largely spread and exceeded the value of prescribed CFRP/concrete bond stress ($\tau_{max} = 4.3$ MPa). Meanwhile, the CFRP sheet has not reached its maximum strain. Similarly, for the beam strengthened by sided bonding scheme B1F-SB, the beam also collapses due to the CFRP delamination, as shown in Fig. 12(b), and the CFRP sheets debonded where the maximum shear stress occurs.

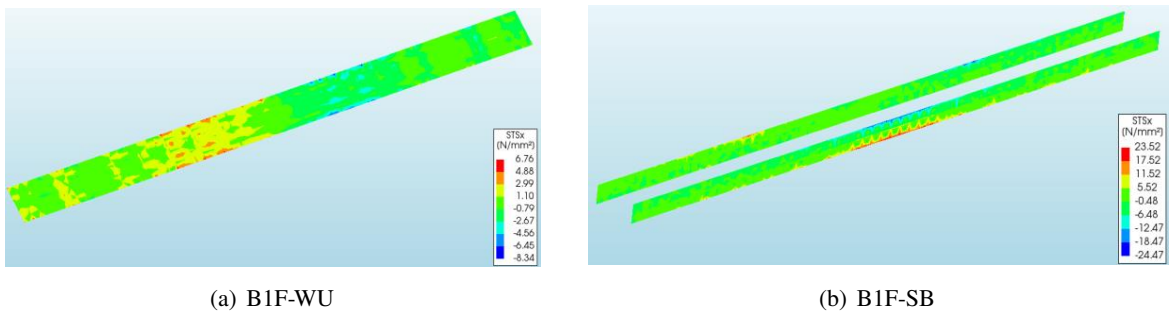


Figure 11. Interfacial shear stress distribution in modeled beams

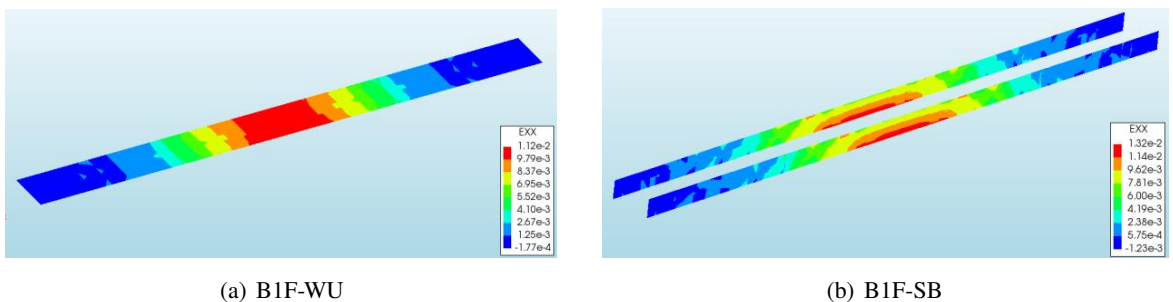


Figure 12. CFRP strain distribution in modeled beams

4.2. Effect of CFRP length and U-wraps

In this section, the CFRP length is explored to investigate its effect on the ultimate flexural strength of strengthened beams. This investigation utilized a CFRP sheet with a length (denoted l)

of 1700 mm in the beam B1F-FEM compared to a reduction to 1350 mm and 900 mm corresponding to 0.75 and 0.5 time of the clear span in the beams named B1F-0.75L and B1F-0.5L, as illustrated in Figs. 13(a) and 13(b). The maximum capacities exhibited higher values than the control beams, which increased by approximately 14.6, 8.9, and 6.4 percent, respectively. Moreover, by taking advantage of U-wraps, the failure status of beams B1F-0.75L and B1F-0.5L, as well as ductility, are kept as with beams B1F.

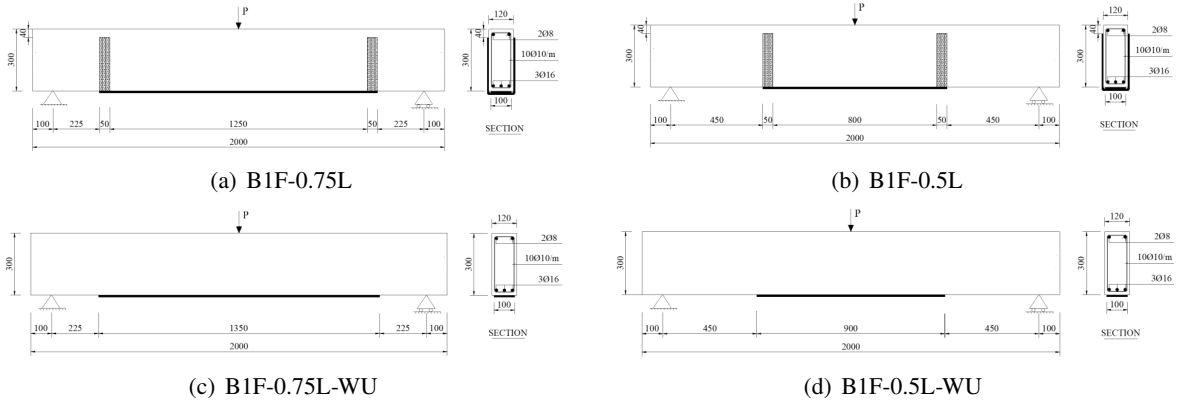


Figure 13. Modeled beams strengthened using different CFRP lengths and with or without U-wraps at the plate ends

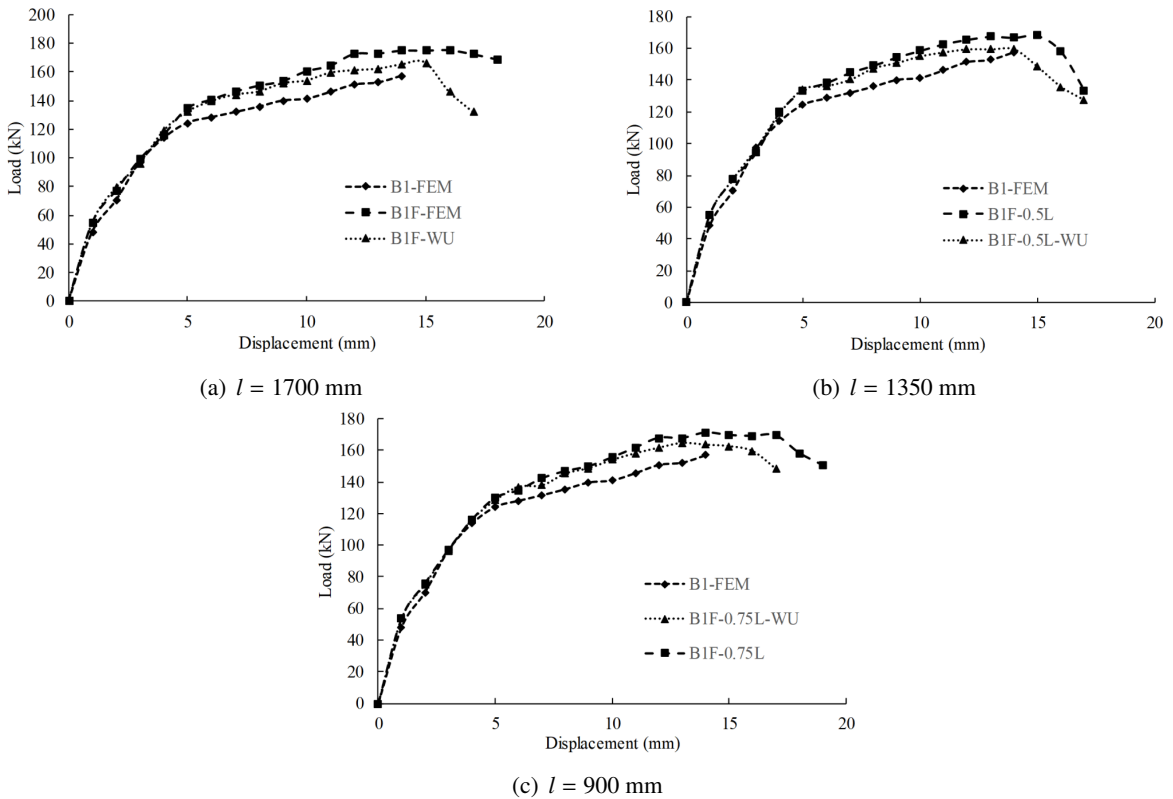


Figure 14. Load-displacement response of beam specimens with different CFRP lengths and anchorage conditions

On the other hand, by eliminating the U-wraps as illustrated in Figs. 9(a), 13(c), and 13(d), the gain in flexural strength is just 5.7, 4.4, and 1.2 percent for beams B1F-WU, B1F-0.75L-WU, and B1F-0.5L-WU. The load-displacement curves obtained in FE analyses are shown in Fig. 14 for each CFRP length studied. In addition, the failure mechanism shifts from a ductile manner to a considerably more brittle manner by transitioning from CFRP rupture to plate end debonding failure. Therefore, the CFRP sheet length can decrease when using U-wraps because of its favorable features in preventing plate end debonding and retaining the ductility of strengthened beam specimens.

4.3. Effect of multiple CFRP layers

In this section, five FE models were investigated for the contribution to the effect of multiple CFRP layers, including the control beam B1-FEM (Fig. 1), the strengthened beam B1F-FEM with a single CFRP layer (Fig. 2), and three strengthened beams named B1F-L2, B1F-L3, and B1F-L5 using 2, 3, and 5 CFRP layers, respectively, as illustrated in Fig. 15. The obtained results from FE analysis show that when increasing the number of CFRP layers from 1 to 5 layers, the predicted load-carrying capacity of the strengthened beams increased by 14.6, 31.2, 34.2, and 42.5% over the control beam B1-FEM, as shown in Fig. 16. In addition, while the increase of CFRP layers enhanced the initial stiffness, the studied beams behave more brittle as the layer number is equal to or larger than three.

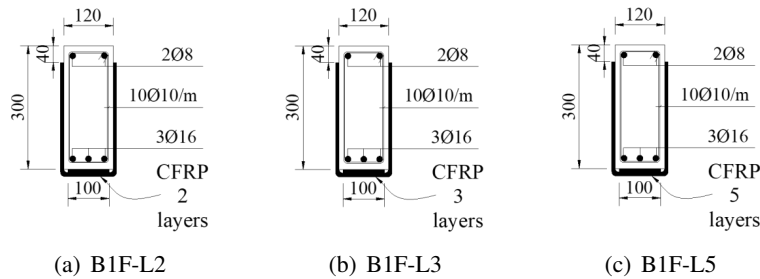


Figure 15. Cross-section of strengthened beams using multiple CFRP layers

As a result of the addition of two CFRP sheets of beam B1F-L2, the strengthened beam increased the ductility significantly over the control beam, which failed with the same mechanism of CFRP sheet rupture as beam B1F-FEM. The failure mechanism was proven in Fig. 17(b) by demonstrating that the strain value of the CFRP sheet produced at the failure step of beam B1F-L2 exceeded its maximum value of 0.0155. For beam specimens with the number of CFRP layers higher than two, the failure mode of strengthened beams shifted from ductile failure with CFRP rupture to CFRP debonding. It is characterized by the concentration of interfacial shear stress in the intermediate span and plate ends of the beam, where the values exceeded the prescribed bond strength ($\tau_{max} = 4.3$ MPa), as shown in Figs. 17(c) and 17(e). In addition, as the number of CFRP sheets increases from 3 to 5, the displacement value of the beam corresponding to the beginning time of CFRP

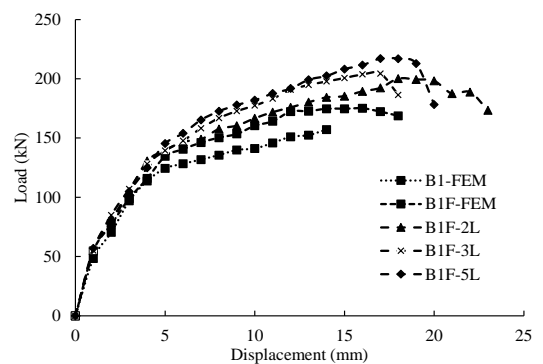


Figure 16. Load-displacement response of beam specimens with multiple layers of CFRP

sheet debonding is both at 17 mm. Therefore, in the case of control beam B1, the number of CFRP strengthening layers should be kept under three to take the most advantage of the performance of the strengthening material, along with maintaining the ductile manner up to a relatively large displacement of strengthened beams.

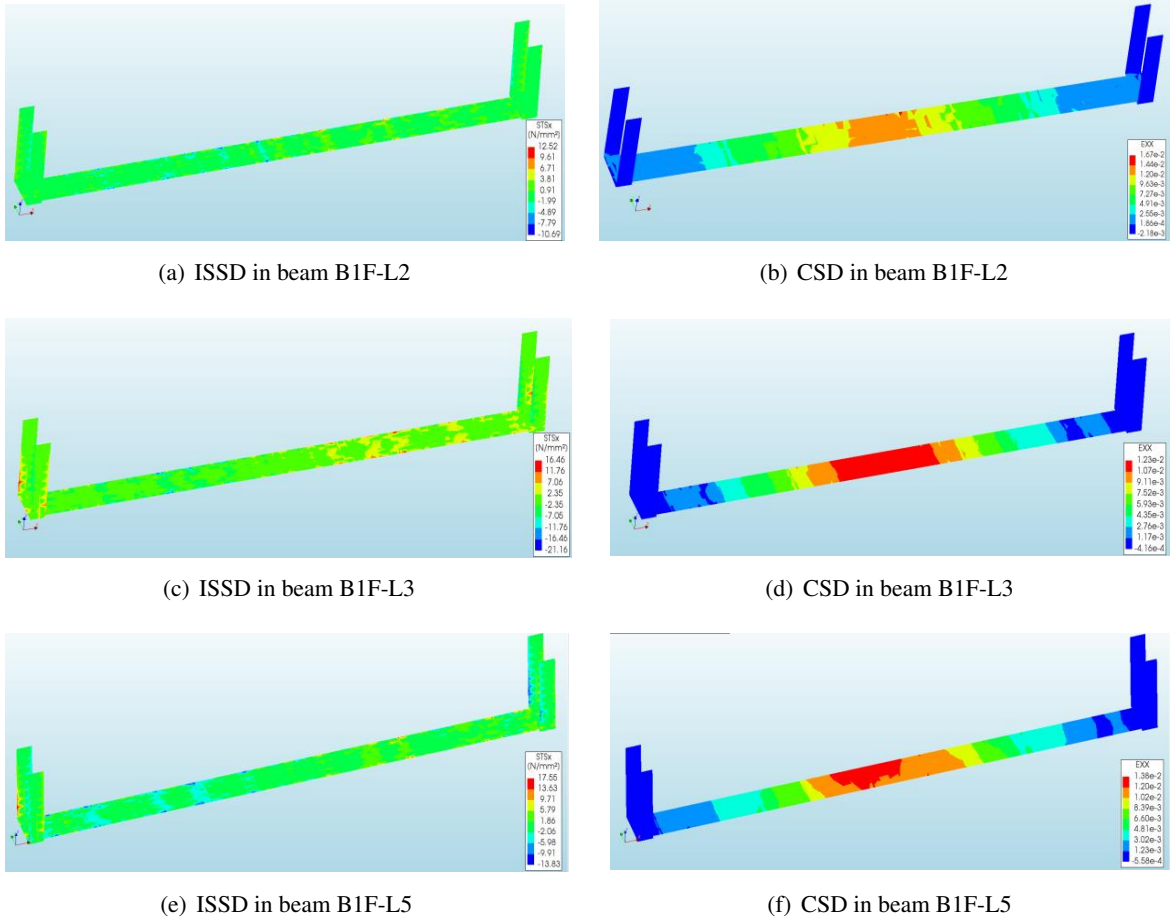


Figure 17. Interfacial shear stress and strain distribution in the longitudinal axis of CFRP sheets

5. Conclusions

The paper shows the results of finite element models to numerically investigate the flexural behavior of RC beams strengthened with externally bonded CFRP sheets. The models were calibrated based on the experimental results of two beam specimens from the research work of El-Ghandour [5]. The results demonstrated a good correlation between the two approaches, especially for obtaining a better prediction of ultimate load. The validated models were then utilized in numerical investigations whose key parameters affecting the flexural performance of strengthened beams are focused, i.e., strengthening schemes, CFRP length, and CFRP layer number. Based on FE analysis results, the following conclusions can be drawn:

- The developed FE model employing bond stress-slip behavior is capable of predicting the flexural capacity of CFRP-strengthened RC beams considering the debonding mechanism.

- In the case of a single CFRP sheet bonded on the bottom surface of the beam, locking the plate ends with U-wraps not only increases the maximum load-carrying capacity by 5.4% but also exploits the full superior tensile strength of the CFRP sheet until rupture. Whereas beam without U-wrap end anchorages, the failure mode obtained was debonding.

- In circumstances where the use of CFRP sheets to strengthen beams is prohibitively costly, the use of U-wraps over the length of CFRP longitudinal reinforcement may be considered. This is due to its favorable properties, which include the ability to prevent plate end debonding and maintain the ductility of strengthened beam specimens.

- By attaching the CFRP sheets to two opposite sides of the beam's web, this strengthening scheme not only simplifies construction but also increases the maximum load capacity with considerable value. However, the increase of strength and overall ductility using this technique showed a limitation compared to the externally bonded scheme with CFRP U-wraps. This is because the failure mode due to CFRP debonding is a waste of material capability.

- When using multiple CFRP layers, even though the failure mode obtained is still unfavorable, i.e., CFRP debonding, the load-carrying capacity of the strengthened beam is significantly improved compared to the control beam. Meanwhile, the strengthened beam remained the ductile behavior with a relatively large displacement. Therefore, it recommends using a limited number of CFRP layers (i.e., three layers in maximum) to strengthen the flexural-critical RC beams to optimize the strength improvement while maintaining the ductility as in the initial design.

Acknowledgment

The authors would like to thank Mr. Du Duc Hieu for his support in the finite element investigations of this study.

References

- [1] Ali, A., Abdalla, J., Hawileh, R., Galal, K. (2014). [CFRP Mechanical Anchorage for Externally Strengthened RC Beams under Flexure](#). *Physics Procedia*, 55:10–16.
- [2] Bahn, B. Y., Harichandran, R. S. (2008). [Flexural behavior of reinforced concrete beams strengthened with CFRP sheets and epoxy mortar](#). *Journal of Composites for Construction*, 12(4):387–395.
- [3] Emarah, D. A. (2019). [Numerical study to investigate the behavior of reinforced concrete slabs with CFRP sheets](#). *Water Science*, 33(1):142–153.
- [4] Al-Tamimi, A. K., Hawileh, R. A., Abdalla, J. A., Rasheed, H. A., Al-Mahaidi, R. (2015). [Durability of the bond between CFRP plates and concrete exposed to harsh environments](#). *Journal of Materials in Civil Engineering*, 27(9):04014252.
- [5] El-Ghandour, A. A. (2011). [Experimental and analytical investigation of CFRP flexural and shear strengthening efficiencies of RC beams](#). *Construction and Building Materials*, 25(3):1419–1429.
- [6] Siddiqui, N. A. (2009). Experimental investigation of RC beams strengthened with externally bonded FRP composites. *Latin American Journal of Solids and Structures*, 343–362.
- [7] Lee, J., Lopez, M. (2020). [Application of Frictional Bond-Slip Model to Large-Scale FRP-Strengthened T-Beams with U-wraps](#). *International Journal of Concrete Structures and Materials*, 14(1):1–15.
- [8] Jeevan, N., Reddy, H. N. J., Prabhakara, R. (2018). [Flexural strengthening of RC beams with externally bonded \(EB\) techniques using prestressed and non-prestressed CFRP laminate](#). *Asian Journal of Civil Engineering*, 19(7):893–912.
- [9] Dong, J., Wang, Q., Guan, Z. (2013). [Structural behaviour of RC beams with external flexural and flexural-shear strengthening by FRP sheets](#). *Composites Part B: Engineering*, 44(1):604–612.
- [10] Pellegrino, C., Modena, C. (2002). [Fiber reinforced polymer shear strengthening of reinforced concrete beams with transverse steel reinforcement](#). *Journal of Composites for Construction*, 6(2):104–111.

- [11] Smith, S. T., Teng, J. G. (2002). [FRP-strengthened RC beams. I: review of debonding strength models.](#) *Engineering structures*, 24(4):385–395.
- [12] Lu, X. Z., Teng, J. G., Ye, L. P., Jiang, J. J. (2005). [Bond–slip models for FRP sheets/plates bonded to concrete.](#) *Engineering structures*, 27(6):920–937.
- [13] Teng, J. G., Yuan, H., Chen, J. F. (2006). [FRP-to-concrete interfaces between two adjacent cracks: theoretical model for debonding failure.](#) *International journal of solids and structures*, 43(18-19):5750–5778.
- [14] Al-Mahaidi, R., Hii, A. K. Y. (2007). [Bond behaviour of CFRP reinforcement for torsional strengthening of solid and box-section RC beams.](#) *Composites Part B: Engineering*, 38(5-6):720–731.
- [15] Godat, A., Chaallal, O., Obaidat, Y. (2020). [Non-linear finite-element investigation of the parameters affecting externally-bonded FRP flexural-strengthened RC beams.](#) *Results in Engineering*, 8:100168.
- [16] Hawileh, R. A., Musto, H. A., Abdalla, J. A., Naser, M. Z. (2019). [Finite element modeling of reinforced concrete beams externally strengthened in flexure with side-bonded FRP laminates.](#) *Composites Part B: Engineering*, 173:106952.
- [17] Ibrahim, A. M., Mahmood, M. S. (2009). Finite element modeling of reinforced concrete beams strengthened with FRP laminates. *European Journal of Scientific Research*, 30(4):526–541.
- [18] Panahi, M., Zareei, S. A., Izadic, A. (2021). [Flexural Strengthening of Reinforced Concrete Beams through Externally Bonded FRP Sheets and Near Surface Mounted FRP Bars.](#) *Case Studies in Construction Materials*, page e00601.
- [19] Saleem, M. U., Khurram, N., Amin, M. N., Khan, K. (2018). [Finite element simulation of RC beams under flexure strengthened with different layouts of externally bonded fiber reinforced polymer \(FRP\) sheets.](#) *Revista de la Construcción. Journal of Construction*, 17(3):383–400.
- [20] Mohamed, O. A., Khattab, R. (2016). [Numerical analysis of reinforced concrete beam strengthened with CFRP or GFRP laminates.](#) In *Key Engineering Materials*, volume 707, Trans Tech Publ, 51–59.
- [21] Jayajothi, P., Kumutha, R., Vijai, K. (2013). Finite element analysis of FRP strengthened RC beams using ANSYS. *Asian Journal of Civil Engineering (Building and Housing)*.
- [22] Hawileh, R. A., Naser, M. Z., Abdalla, J. A. (2013). [Finite element simulation of reinforced concrete beams externally strengthened with short-length CFRP plates.](#) *Composites Part B: Engineering*, 45(1): 1722–1730.
- [23] Salama, A. S. D., Hawileh, R. A., Abdalla, J. A. (2019). [Performance of externally strengthened RC beams with side-bonded CFRP sheets.](#) *Composite Structures*, 212:281–290.
- [24] Sobuz, H. R., Ahmed, E., Uddin, M. A., Hasan, N. M. S., Uddin, M. J. (2011). Structural strengthening of RC beams externally bonded with different CFRP laminates configurations. *Journal of Civil Engineering (IEB)*, 39(1):33–47.
- [25] Ferreira, D., Manie, J. (2020). *DIANA Documentation release 10.3.* DIANA FEA bv, The Netherlands.
- [26] Model Code 2010 (2013). *fib Model Code for Concrete Structures 2010.* Ernst & Sohn, Berlin, Germany.
- [27] Nakamura, H., Higai, T. (2001). Compressive fracture energy and fracture zone length of concrete. In *Modeling of inelastic behavior of RC structures under seismic loads*, ASCE, 471–487.
- [28] Hordijk, D. A., Reinhardt, H. W. (1993). [Numerical and experimental investigation into the fatigue behavior of plain concrete.](#) *Experimental Mechanics*, 33(4):278–285.
- [29] Rots, J. G. (1991). [Smeared and discrete representations of localized fracture.](#) *International Journal of Fracture*, 51(1):45–59.